Spectral-Domain Covariance Estimation with A Priori Knowledge

PRASHANTH R. GURRAM

NATHAN A. GOODMAN, Member, IEEE
The University of Arizona

A knowledge-aided spectral-domain approach to estimating the interference covariance matrix used in space-time adaptive processing (STAP) is proposed. Prior knowledge of the range-Doppler clutter scene is used to identify geographic regions with homogeneous scattering statistics. Then, minimum-variance spectral estimation is used to arrive at a spectral-domain clutter estimate. Finally, space-time steering vectors are used to transform the spectral-domain estimate into a data-domain estimate of the clutter covariance matrix.

The proposed technique is compared with ideal performance and to the fast maximum likelihood technique using simulated results. An investigation of the performance degradation that can occur due to various inaccurate knowledge assumptions is also presented.

Manuscript received December 21, 2004; revised May 25, 2005; released for publication February 8, 2006.

IEEE Log No. T-AES/42/3/884470.

This work was supported in part by DARPA and AFRL under Contract FA8750-04-1-0110.

Authors' current addresses: P. R. Gurram, Qualcomm, Inc., San Diego, CA 92121, E-mail: (pgurram@qualcomm.com); N. A. Goodman, Dept. of Electrical and Computer Engineering, The University of Arizona, Tucson, AZ 85721, E-mail: (goodman@ece.arizona.edu).

I. INTRODUCTION

A primary objective of airborne radar is to detect targets in the presence of interference such as ground clutter, noise, and jamming. In practice, these interference signals can dominate target signals; therefore, target detection requires signal-processing techniques such as space-time adaptive processing (STAP) [1–6]. STAP exploits the specific structure of ground clutter in the two-dimensional (2-D) angle-Doppler domain to distinguish moving targets from ground clutter and other interference.

Traditionally, STAP is performed by estimating interference statistics from secondary training data taken from range bins near to, but not including, the range bin under test (RUT). This is intuitively satisfying since range bins that are in geographic proximity to the RUT are expected to be statistically similar to the RUT. Unfortunately, it has been shown in [7] that significant secondary sample support, on the order of twice the number of space-time measurements, is required to achieve an average signal-to-interference-plus-noise ratio (SINR) loss of 3 dB relative to ideal, known-covariance performance. With this amount of required training data, it is inevitable that at least some range bins used for training will contain an angle-Doppler clutter spectrum that is significantly different from the RUT.

These problems of sample support and data heterogeneity have motivated the development of reduced-order methods [1, 8–11], structured-covariance methods [12–15] and knowledge-aided methods [16–20]. Reduced-order methods improve performance in situations where the space-time interference covariance matrix must be estimated from a limited amount of training data. Structured covariance methods significantly enhance STAP performance by reducing the amount of sample support required when partial information about the interference covariance matrix is known a priori. For example, the fast maximum likelihood (FML) approach of [14] reduces the training data requirement by reasonably assuming the power and structure of white receiver noise.

We present an alternative training method, originally summarized in [20], that incorporates a priori estimates of the scattering background for use in heterogeneous clutter environments. It has already been demonstrated that knowledge sources such as digital elevation maps, land cover databases, roadmaps, and other known features can be used to compute high-fidelity estimates of observed ground clutter [21–22]. Based on this modeling capability, we propose a spectral-domain approach to estimating the interference covariance matrix used in STAP. A priori modeling of the clutter profile is used in cooperation with real-time data to estimate clutter in the range-Doppler domain. This approach enables

clutter averaging over statistically similar scattering regions rather than over range bins that are often statistically dissimilar. Once the range-Doppler clutter profile is estimated, it is transformed to the clutter covariance matrix based on known space-time steering vectors. In practice, only limited knowledge of the radar system's parameters and flight geometry is available. Therefore, in addition to the ideal performance of the proposed technique, the work presented here also explores and characterizes the effects of some potential errors in the assumptions made and presents examples of how real-time data might be used to minimize these errors. The clutter background used here for the simulations are more realistic and have a higher dynamic range than the clutter background used in [20]. This has motivated development of the minimum-variance estimation presented here. Moreover, the analysis here includes ICM effects and narrowband channel mismatch, which were not evaluated in [20].

In the following sections, we describe our proposed technique and compare performance with ideal, known-covariance performance and with the FML approach of [14]. In Section II, the assumed signal model is summarized. In Section III, the knowledge-aided spectral-domain approach to covariance estimation is described. In Section IV, a minimum-variance range-Doppler image formation technique is presented. This technique improves range-Doppler clutter estimation through the use of a priori modeling of the clutter scene. In Section V, simulation results are presented to demonstrate the performance of the proposed spectral-domain covariance estimation. Errors in a priori knowledge are also investigated. Conclusions are made in Section VI.

II. SIGNAL MODEL AND STAP FUNDAMENTALS

Let the radar system transmit a coherent pulse train. The signal from a point scatterer at cross-range position f_x arriving at an antenna at position $\mathbf{r}$ is a scaled and delayed version of the transmitted signal, which is down-converted and matched filtered to produce a baseband received signal of

$$\tilde{x}(\mathbf{r},t,f_x) \approx \gamma_0(f_x)e^{-j\omega_c\tau(\mathbf{r},t,f_x)} \tag{1}$$

where $\tau(\mathbf{r},t,f_x)$ is the two-way propagation delay that depends on space, slow time, and scatterer position and $\gamma_0(f_x)$ is a complex random variable that accounts for propagation loss, antenna patterns, scatterer reflectivity, and other factors.

While (1) represents the signal received from a single scatterer, the complete space-time signal measured by the radar is due to all scatterers within a constant range contour. To obtain this signal, the point scatterer response in (1) is integrated over the entire range bin of interest. Denoting R_x as the iso-range contour of interest within the area illuminated by the radar's transmit beam gives

$$d_c(\mathbf{r},t) = \int_{R_x} \gamma_0(f_x)e^{-j\omega_c\tau(\mathbf{r},t,f_x)}df_x \tag{2}$$

where the subscript c denotes that this is the contribution due to ground clutter. For simulation purposes, the cross-range dimension is divided into cells, called clutter patches, and the integral is approximated with a summation. If the effective reflection coefficient accounting for all scatterers (and all other amplitude and phase terms such as the antenna patterns and propagation loss) within the ith clutter patch is $\gamma(f_{x_i})$, then the discrete signal model for clutter is

$$d_c(\mathbf{r},t) = \sum_{i=1}^{N_c} \gamma(f_{x_i})e^{-j\omega_c\tau(\mathbf{r},t,f_{x_i})} \tag{3}$$

where N_c is the number of patches in the constant-range contour R_x.

Finally, the radar samples the received signal at multiples of the pulse repetition interval at each antenna element. If there are M pulses and N antennas, then the radar collects MN space-time measurements defined by

$$d_c(n,m) = \sum_{i=1}^{N_c} \gamma(f_{x_i})e^{-j\omega_c\tau(\mathbf{r}_n,t_m,f_{x_i})} \tag{4}$$

where $\mathbf{r}_n$ is the position of the nth antenna element for $0 \le n \le (N-1)$ and $t_m = mT_R$ for $m \le 0 \le (M-1)$. The space-time steering vector $\mathbf{v}(f_{x_i})$ is defined by stacking space-time samples of the complex exponential in (4),

$$\mathbf{v}(f_{x_i}) = [e^{-j\omega_c\tau(\mathbf{r}_1,t_1,f_{x_i})} \quad e^{-j\omega_c\tau(\mathbf{r}_1,t_2,f_{x_i})} \ldots \quad e^{-j\omega_c\tau(\mathbf{r}_1,t_{M-1},f_{x_i})} \ldots e^{-j\omega_c\tau(\mathbf{r}_{N-1},t_{M-1},f_{x_i})}]^T \tag{5}$$

where $(\cdot)^T$ denotes the transpose operation. The space-time clutter snapshot, $\mathbf{d}_c$, for a single range bin is

$$\mathbf{d}_c = \sum_{i=1}^{N_c} \gamma(f_{x_i})\mathbf{v}(f_{x_i}). \tag{6}$$

It is well known that the optimum weight vector used to test for the presence of a target is [1–4]

$$\mathbf{w} = k\mathbf{R}_I^{-1}\mathbf{s} \tag{7}$$

where k is an arbitrary constant, $\mathbf{s}$ is the space-time steering vector for a target at a given azimuth location and Doppler shift, and $\mathbf{R}_I$ is the interference covariance matrix. In practice, the interference covariance matrix must be estimated with training data. Data-domain techniques require averaging over range, but unfortunately, poor performance often results due to nonstationarity of the training

data. In reality, the angle-Doppler power spectrum of ground clutter varies with range due to varying clutter background or other factors. Furthermore, additional targets within the training region can corrupt the covariance estimate [21], and aircraft crab [1] and nonlinear arrays [23] cause the space-time clutter ridge to vary with range. Some discussions of real-world effects and their impacts on STAP performance can be found in [2].

Although data-domain covariance estimates can be corrupted by heterogeneity of the training data, they have some definite benefits that should be mentioned. Because the interference statistics are estimated from real-time data, any jammers that are present will also be estimated in the training process. Hence, data-domain techniques inherently estimate the statistics of clutter, additive noise, and jammers in a single well-defined process. Furthermore, channel mismatches and other uncalibrated system characteristics are inherently included in the covariance estimation, although mismatches will still be present in the target steering vector, **s**.

The FML approach that we use for comparison also has these advantages, but in addition, the FML approach effectively uses realistic information about the thermal noise covariance matrix to significantly enhance the convergence performance of STAP. In [14], the interference covariance matrix is separated into an unknown matrix describing colored interference and a known matrix representing white noise. The maximum likelihood estimate of the unknown matrix is derived, and since the estimation is of the lower-rank matrix of colored interference, convergence is much improved. It was shown in [14] that the FML approach performs significantly better than the sample covariance matrix when factors such as clutter heterogeneity limit the amount of useful training data. The proposed spectral-domain technique is compared here with ideal performance and with the performance of the FML technique.

III. KNOWLEDGE-AIDED SPECTRAL AVERAGING APPROACH

We now propose an alternative technique for computing the interference covariance matrix used in STAP. In the following, we emphasize that range-Doppler processing inherently provides an estimate of ground clutter, and we maintain that the range-Doppler domain is a natural domain for applying knowledge sources that typically provide information as a function of geographic location on the Earth.

Consider the correlation between two measurements of ground clutter that are separated in both time and space by the quantities ν and χ, respectively. Using (2), this correlation is

$$\begin{aligned} R_c(\chi,\nu) &= \mathrm{E}[d_c(\mathbf{r},t)d_c^*(\mathbf{r}+\chi,t+\nu)] \\ &= \mathrm{E}\left[\int_{R_x}\gamma_0(f_x)e^{-j\omega_c\tau(\mathbf{r},t,f_x)}df_x\int_{R_x}\gamma_0^*(f')e^{j\omega_c\tau(\mathbf{r}+\chi,t+\nu,f')}df'\right] \\ &= \iint_{R_x}\mathrm{E}[\gamma_0(f_x)\gamma_0^*(f')]e^{-j\omega_c\tau(\mathbf{r},t,f_x)}e^{j\omega_c\tau(\mathbf{r}+\chi,t+\nu,f')}df'df_x \end{aligned} \tag{8}$$

where the asterisk operator denotes complex conjugate. In (8), the expected value operator can be restricted to the reflectance variables since they are the only random quantities—the complex exponentials are known for a given geometry and set of radar parameters. Assuming that the complex reflectance is uncorrelated for scatterers at different locations, the expected value in (8) becomes

$$\mathrm{E}[\gamma_0(f_x)\gamma_0^*(f')] = \sigma_o^2(f')\delta(f_x - f') \tag{9}$$

where $\sigma_o^2(f')$ is the position-dependent radar cross section (RCS) density of the background within the range bin and $\delta(f)$ is the Dirac delta function. Substituting (9) into (8) and simplifying yields

$$\begin{aligned} R_c(\chi,\nu) &= \iint_{R_x}\sigma_o^2(f')\delta(f_x-f')e^{-j\omega_c\tau(\mathbf{r},t,f_x)}e^{j\omega_c\tau(\mathbf{r}+\chi,t+\nu,f')}df'df_x \\ &= \int_{R_x}\sigma_o^2(f_x)e^{-j\omega_c\tau(\mathbf{r},t,f_x)}e^{j\omega_c\tau(\mathbf{r}+\chi,t+\nu,f_x)}df_x. \end{aligned} \tag{10}$$

Equation (10) is a continuous version of the traditional space-time clutter covariance model. The clutter covariance matrix contains every space-time lag sampled by the radar system:

$$\mathbf{R}_c = \mathrm{E}[\mathbf{d}_c\mathbf{d}_c^H] \tag{11}$$

where the superscript H denotes conjugate transpose. Substituting (6) into (11) and proceeding similar to the steps for (8)–(10) gives

$$\begin{aligned} \mathbf{R}_c &= \sum_{i=1}^{N_c}\sigma_c^2(f_{x_i})\mathbf{v}(f_{x_i})\mathbf{v}(f_{x_i})^H \\ &= \sum_{i=1}^{N_c}\sigma_i^2\mathbf{v}_i\mathbf{v}_i^H \end{aligned} \tag{12}$$

where $\sigma_i^2 = \sigma_c^2(f_{x_i})$ is the expected power contribution from the ith clutter patch.

Equation (10) represents the space-time autocorrelation function of the clutter random process. The function $\sigma_o^2(f')$ is a power spectral density (PSD) that describes the expected power of ground clutter reflections as a function of cross-range position for a given range bin. Hence, clutter can be estimated either in the space-time data domain via the sample covariance matrix or FML, or through spectral estimation in the frequency domain via

(12). The spectral-domain approach corresponds to the process of estimating clutter power versus cross-range position. Since cross-range can be mapped to specific geographic locations on the Earth's surface for a known flight geometry, the spectral domain is a logical domain for applying a priori knowledge sources to improve clutter estimation. This is because many possible knowledge sources provide their information as a function of position on the Earth; therefore, performing clutter estimation in the spectral or range-Doppler domain provides an opportunity to register a priori knowledge with data-derived clutter estimates. It also enables clutter to be averaged geographically in a manner that is consistent with land cover type, terrain slope, and other factors rather than averaging over range bins that may or may not be statistically consistent.

The spectral-domain approach involves computing the clutter covariance matrix using (12) rather than by averaging snapshots in the data domain. We note that range-Doppler processing inherently provides a spectral estimate of ground clutter—it creates a map of stationary-scatterer reflected power versus range and Doppler. But unfortunately, the values in a range-Doppler image cannot be used in (12) directly due to the speckle phenomenon. That is, each pixel in a range-Doppler map represents the sum of many scatterers within a resolution cell; hence, a single range-Doppler image pixel is probably not equal to its statistical average. This is consistent with the expected value operator in (9), which says the PSD must be an averaged estimate. Fortunately, if multiple resolution cells from the same surface type are available, they can be averaged to get an accurate value of that surface's RCS. For example, if the boundaries of a grassland, lake, or agricultural area could be identified, the scattering from all range-Doppler cells within the boundaries of one of these features is expected to adhere to the same probability distribution. If the boundaries of such homogeneous regions, or segments, can be identified using knowledge sources such as digital elevation databases, land cover databases, and prior synthetic aperture radar (SAR) surveys, then all cells within the boundaries can be averaged. Then, each cell can be replaced with its region's average reflected power for use as a clutter patch power coefficient in (12). In heterogeneous scattering environments, the terrain statistics may vary dramatically over small changes in range. Therefore, it makes more sense to average over surface types having the same probability distribution in the spectral domain than it does to average over dissimilar range bins in the data domain.

Of course, in order to transform between the spectral and data domains, we see in (12) that space-time steering vectors are needed. Under ideal circumstances, these steering vectors can be computed based on available ownship data and knowledge of the flight geometry, but in practice, performance can be sensitive to even small errors in these parameters. This, in turn, places strong requirements on the accuracy of ownship and scenario knowledge. The ultimate efficacy of the proposed approach will depend on the accuracy with which radar parameters and scenario features can be predicted or estimated. In a subsequent section, we analyze the performance effects of a few specific cases of imprecise knowledge such as inaccurate crab angle, inaccurate wind speed in an assumed ICM model, and narrowband (NB) channel mismatch due to imperfectly calibrated spatial channels.

A summary of the proposed technique is given as follows.

1) Knowledge sources are used to model the observed clutter scene for a predicted flight profile. The output of the modeling is an RCS map versus range and cross-range.
2) Homogeneous scattering regions are identified in the modeled clutter scene. This is performed by image-processing techniques such as median filtering and edge detection applied to the modeled scene.
3) The radar collects data and forms a range-Doppler image. In our results, we use minimum-variance spectral estimation to form the image.
4) This image is then segmented using the information from step 2 above to isolate homogeneous scattering regions.
5) Within each homogeneous segment, all pixels are replaced by the segment's average to obtain the estimated clutter power profile for use in (12). Compensation for antenna patterns is included during averaging, but R^4 and grazing angle variations are negligible within individual segments.
6) The collected data are used to correct imprecise knowledge that could corrupt the computation of the space-time steering vectors for each clutter patch. For example, collected data can be used to estimate platform crab angle.
7) The interference covariance matrix is calculated using (12).

Fig. 1 shows a block diagram of the proposed processing approach.

IV. MINIMUM-VARIANCE RANGE-DOPPLER FILTERING

Range-Doppler processing provides an estimate of ground clutter by creating a map of stationary-scatterer reflected power versus range and azimuth. The simplest method for generating a range-Doppler image is to compute the discrete Fourier transform of the pulses for each range

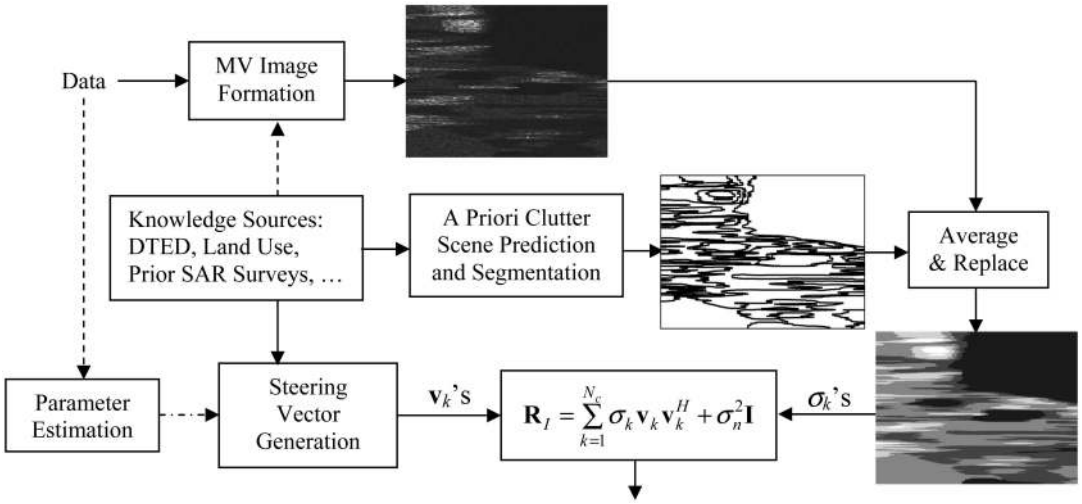

Fig. 1. Block diagram of the proposed knowledge-aided spectral-averaging approach.

bin. Unfortunately, while this technique may be sufficient for basic range-Doppler imaging or as the foundation for SAR imaging, it does not produce a spectral estimate that is sufficient for forming a clutter covariance matrix. There are two reasons why Fourier-based imaging is insufficient for this purpose. First, when the clutter background has a high dynamic range (high-RCS regions adjacent to low-RCS regions), clutter power from stronger regions will leak into resolution cells of weaker regions through sidelobes of the Doppler filters and range compression. Window functions can reduce these sidelobes, but the tradeoff in resolution may be unacceptable since in STAP we are already starting with short processing intervals. The second reason that Fourier-based range-Doppler imaging is insufficient is that thermal noise biases regions of low clutter power. Consider a region that should have negligible backscatter. Resolution cells corresponding to this region in the range-Doppler clutter map should be nearly zero, but the imaging process will produce a non-zero result due to the presence of white receiver noise. Even if resolution is improved or if the dynamic range of the clutter background isn't enough to make Doppler sidelobes an issue, noise will still bias the spectral estimates for low-RCS regions. Hence, when attempting to detect targets in these low-clutter regions, the STAP filter will be mismatched and the clutter will be overnulled.

To overcome these problems, a minimum-variance range-Doppler image formation technique has been developed. This technique incorporates a priori modeling of the clutter background directly into a minimum-variance estimate of the clutter scene. We derive this technique in the following discussion.

A. Minimum-Variance Filter Derivation

The temporal data from a single spatial channel is used to compute the range-Doppler clutter estimate. Let k represent the current clutter patch (the patch under test) whose power is being estimated. Let $\mathbf{u}_k = \mathbf{u}(f_{x_k})$ be the temporal steering vector for the kth clutter patch. The minimum-variance spectral estimator for the kth patch, $\mathbf{w}_k$, is found by solving

$$\min_{\mathbf{w}_k} \mathbf{w}_k^H \mathbf{R}_t \mathbf{w}_k \tag{13}$$

subject to the constraint $\mathbf{w}_k^H \mathbf{u}_k = 1$. In (13), $\mathbf{R}_t$ is the a priori temporal covariance matrix

$$\mathbf{R}_t = \sum_{i=1}^{N_c} \sigma_i^2 \mathbf{u}_i \mathbf{u}_i^H + \sigma_n^2 \mathbf{I} \tag{14}$$

where σ_i^2 is the a priori estimate of the power from the ith patch as in (12). The solution is

$$\mathbf{w}_k = \sigma_k^2 \mathbf{R}_t^{-1} \mathbf{u}_k \tag{15}$$

which leads to

$$\mathbf{w}_k = \sigma_k^2 \left(\sum_{i=1}^{N_c} \sigma_i^2 \mathbf{u}_i \mathbf{u}_i^H + \sigma_n^2 \mathbf{I} \right)^{-1} \mathbf{u}_k. \tag{16}$$

The filter defined by (16) is very similar to the optimum detection filter for STAP, except that the covariance matrix is obtained from a priori knowledge and the target steering vector is a temporal vector for a clutter patch rather than space-time vector for a moving target.

B. Performance of Minimum-Variance Filter

Fig. 2 demonstrates the performance of the minimum-variance range-Doppler filtering based on the clutter background for the first KASSPER datacube [24]. More details about how this datacube was used are given in the following section. In Fig. 2(a), we see that the true range-Doppler clutter

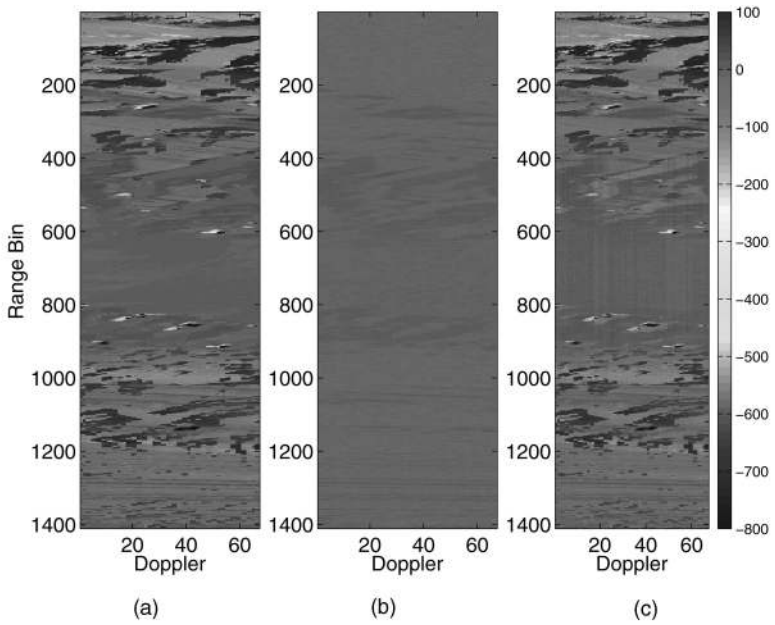

Fig. 2. (a) Original range-Doppler power profile of clutter along with (b) Fourier-based range-Doppler image and (c) Minimum-variance-based range-Doppler image.

profile has a dynamic range of over 800 dB. Note that this is not the dynamic range of the radar, but the dynamic range of the background that is input into the simulation. Because of the high dynamic range, there are very low power regions adjacent to very high power regions. In Fig. 2(b), we clearly see the effects of this dynamic range on the output of the Fourier-based range-Doppler image. The low-power regions have been washed out by sidelobe leakage and noise corruption, which leads to overnulling. In Fig. 2(c), we see that the minimum-variance range-Doppler image does an excellent job of reconstructing the original clutter power profile. Of course, the radar cannot measure an 800 dB dynamic range. The estimated power for every patch, however, is a function of both collected data and a priori knowledge. In regions where the reflected power is extremely low, the minimum-variance estimator believes the a priori knowledge more than the noisy data. This is easily confirmed by noting that the magnitude of $\mathbf{w}_k$ in (16) is proportional to the kth patch's a priori power estimate.

V. SIMULATIONS AND RESULTS

In this section, we demonstrate the potential performance of our spectral-based covariance estimation compared to known-covariance performance and FML performance. The FML method [14] was simulated with the true noise covariance matrix as the initial estimate and with sample support of 100 snapshots. First, performance is compared under perfect a priori knowledge assumptions. Then, the effects of various errors in knowledge are investigated. We study the effects of inaccurate platform crab angle, of mismatched wind speed when accounting for ICM, and of NB channel mismatch resulting from imperfect calibration. This analysis shows that of these factors, inaccurate crab angle can degrade performance the most. An example of using real-time data to estimate unknown platform crab angle is also demonstrated.

Since the spectral-domain technique involves identification and averaging of homogeneous scattering regions, it is most useful for higher resolution scenarios where varying clutter background can be observed and segmented within the radar's main beam. Therefore, the simulation used to produce the results in this section is based on the RCS background from the publicly released first KASSPER data set [24], but the data has been resimulated at higher resolution and does not include every error effect that was in the original data set. The range/cross-range clutter background from the first KASSPER data set was used as the clutter power input to our own STAP simulation. We convert the background patch powers to random complex reflectances and compute the datacube. ICM is added to the ideal and knowledge-aided covariance matrices using covariance matrix tapers (CMT) [25–27] and added to the simulated datacube with a corresponding random temporal modulation. Likewise, NB channel mismatch is added to covariance matrices with a rank-one CMT and is added to the datacube through channel-dependent amplitude and phase terms [2].

The simulation parameters are as follows. The radar is flying at an altitude of 3000 m looking

sideways at an elevation angle of $-5°$. The radar operates at 1240 MHz with a bandwidth of 10 MHz. The antenna array has 11 elements. On transmit, the array elements operate coherently to produce a directed narrow beam. On receive, each array element collects and samples the received signal independently. The radar velocity is 200 m/s, the pulse-repetition frequency (PRF) is 900 Hz, and the number of pulses in a coherent processing interval (CPI) is 64. These parameters yield a CPI that is four times longer than the original KASSPER data set. ICM corresponds to the Billingsley exponential decay model [28] with a wind speed of 15 mi/h and β parameter of 5.7. Where appropriate, NB channel mismatch is modeled with random gain and phase factors for each channel [2]. The simulated datacube consisted of noisy space-time data for $2MN$ range bins plus the RUT and a few guard cells. In the simulation results provided below, SINR performance is generalized by averaging over a set of range bins. This approach is taken because SINR results for any single range bin can be misleading if there is accidental similarity between that range's clutter spectrum and the average clutter spectrum of the training data.

A. Performance Under Perfect Knowledge

Figs. 3 and 4 show the performance of spectral-domain averaging under accurate knowledge assumptions. The ideal clutter background was processed with an image-processing program to obtain the boundaries around homogeneous regions of similar power. The image-processing program smoothed the clutter background with a three-pixel by three-pixel median filter, segmented the background with the Sobel edge detector [29], and averaged the pixels within each segment. The clutter background was also used as a priori knowledge for the minimum-variance range-Doppler image formation. It is assumed that the space-time steering vectors needed to transform from the range-Doppler domain to the clutter covariance matrix are known perfectly. Hence, after averaging the range-Doppler estimate, the estimated clutter and noise covariance matrices are computed and SINR performance is evaluated. Fig. 3 shows SINR performance averaged over range bins 264 through 292. It can be seen in Fig. 3 that spectral-domain averaging performs very well. In Fig. 4, another set of range bins from 420 through 470 is tested and it is observed that spectral-domain averaging outperforms the FML approach. The major improvement is possible in this case because the clutter in range bins 420 through 470 is relatively weak, but other range bins within the training range contain strong clutter. Hence, clutter needs to be only partially rejected. But because data-domain techniques include range bins in the training data that have very high clutter power, their estimated covariance

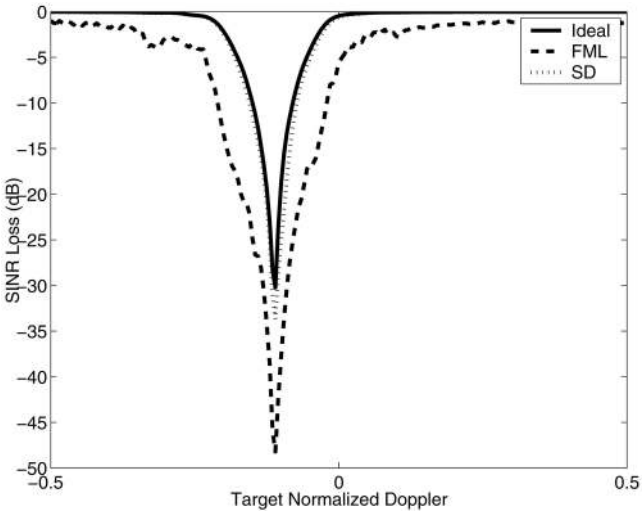

Fig. 3. Average SINR performance over first set of range bins, [264 : 292], under conditions of perfect knowledge.

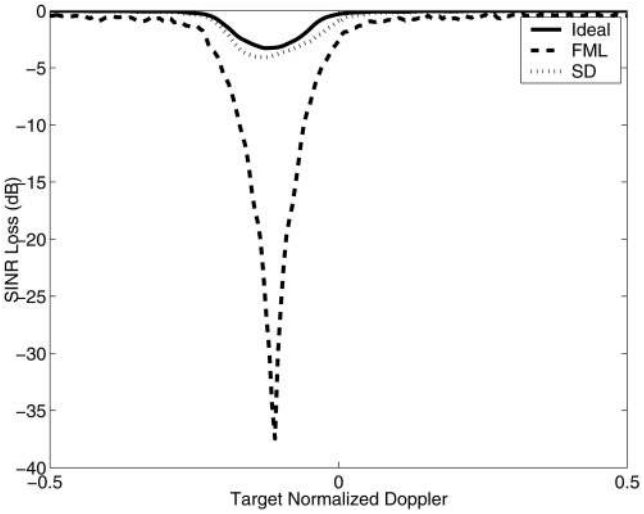

Fig. 4. Average SINR performance over second set of range bins, [420 : 470], under conditions of perfect knowledge.

matrices contain too much clutter power. The result is that FML severely overnulls clutter although it certainly performs better than a traditional, slowly converging approach. Spectral-domain averaging with prior knowledge, however, makes a distinction between clutter regions with different average power. High-power range bins have not contributed to the average for the RUT; therefore, the clutter estimate is much more accurate and excellent results are achieved. All subsequent results are based on the first set of range bins: [264–292].

In generating Figs. 3 and 4, perfect knowledge of the ideal clutter background was assumed for purposes of generating homogeneous region boundaries and for computing the range-Doppler filters. It was also assumed that the space-time steering vectors for each clutter patch were known exactly. This implies exact knowledge of the flight scenario, the true aircraft crab, and the individual channel calibrations. The

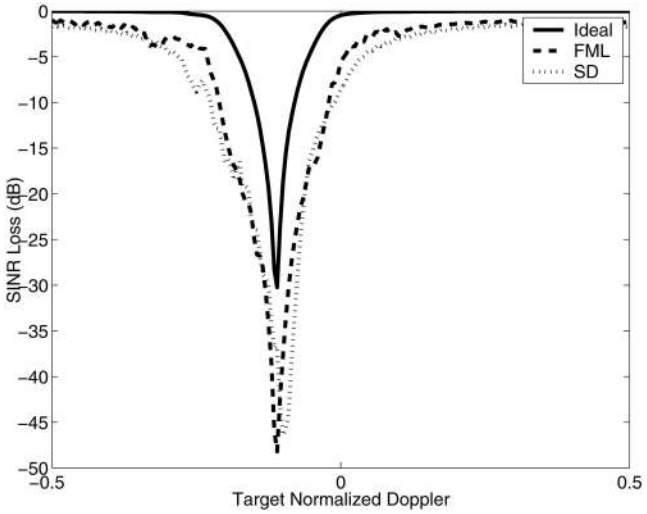

Fig. 5. Average SINR loss for case of incorrect platform crab knowledge.

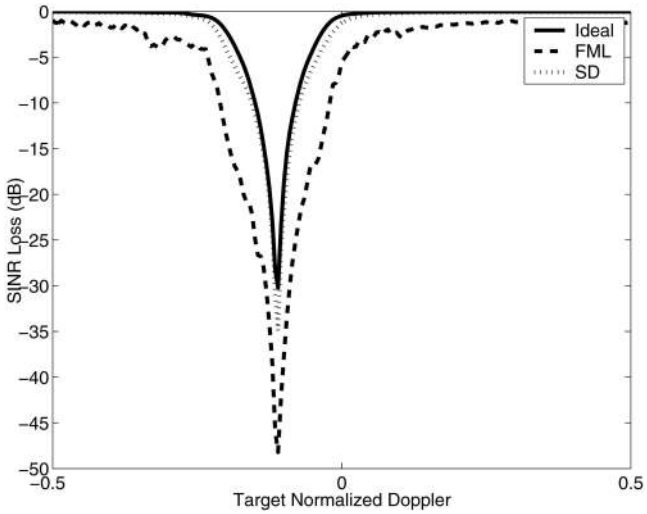

Fig. 6. Average SINR loss for case of imperfect ICM knowledge.

true wind speed and clutter type were used to apply a CMT account for ICM and the NB channel mismatch was set to zero. Finally, an accurate noise covariance matrix was added to the clutter covariance matrix.

B. Effects of Imperfect Knowledge

In practice, many of the above assumptions will be invalid. In the following, we present results for situations where our assumed knowledge does not agree with reality. In the first case, the effects of a mismatched velocity vector are studied. For Fig. 5, all the parameters are identical to Fig. 4 except for a mismatch in the assumed platform crab angle. In producing Fig. 5, the datacube was generated for a platform with an actual crab angle of 3.5°. In computing the space-time steering vectors necessary for transforming the clutter power coefficients to the clutter covariance matrix, it was assumed that the platform's crab angle was 3°. This mismatch causes an incorrect mapping from the range-Doppler domain to the space-time data domain, and SINR performance is degraded as seen in Fig. 5 due to a displaced clutter null. Actually, the presence of ICM has reduced the sensitivity to inaccurate crab, but there is still enough mismatch to degrade performance. In this case, the clutter PSD has been estimated very well, but the covariance matrix is inaccurate due to a flawed spectral-domain to data-domain transformation.

Fig. 6 demonstrates the effect of imperfect ICM on SINR performance. In producing Fig. 6, the true wind speed was 15 mi/h while the assumed wind speed was 2 mi/h. Spectral-domain averaging performs well even for this large amount of mismatch in ICM wind speed. This implies that spectral-domain averaging is somewhat insensitive to incorrect ICM modeling as long as some ICM is present in reality and in the modeling. Precise ICM modeling does not appear to be required.

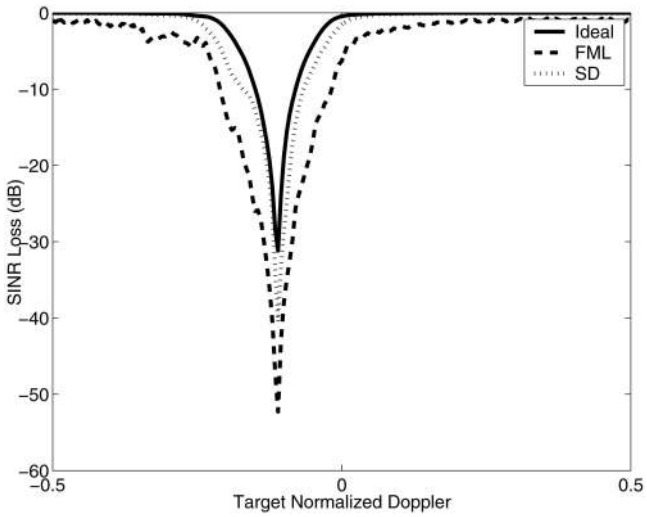

Fig. 7. Average SINR loss for case of unknown NB channel mismatch.

In Fig. 7, imperfect channel calibration is investigated. The incorrect channel calibration is modeled as a NB channel mismatch, which modifies the measurements with a different amplitude and phase for each channel. In producing Fig. 7, the true variation in gain and phase are between $0.97 \leq \varepsilon_i \leq 1$ and $-4° \leq \phi_i \leq 4°$, respectively, whereas, perfect channel calibration is assumed in applying the spectral-domain to data-domain transformation ($\varepsilon_i = 1$ and $\phi_i = 0°$). From Fig. 7, imperfect NB channel mismatch has some effect on spectral-domain averaging, but the observed degradation is less than what is observed for incorrect crab angle.

Fig. 8 shows performance when all three previous errors are present. Crab angle, ICM wind speed, and channel calibration are all inaccurate. In performing this simulation, these effects are combined to see the overall degradation. Comparing Figs. 5, 6, and

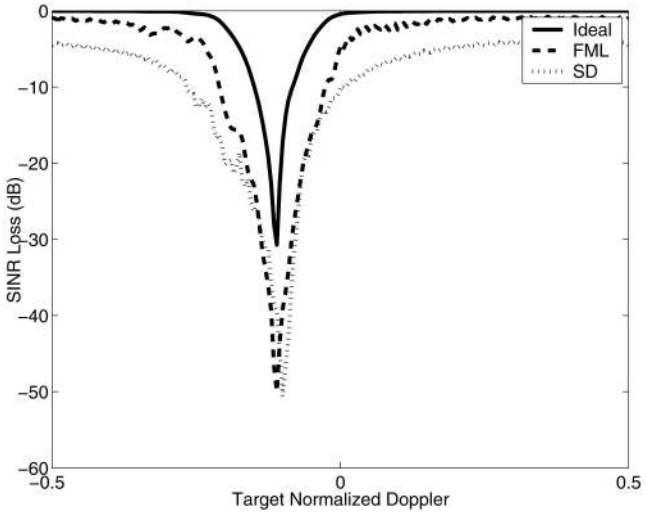

Fig. 8. Average SINR loss for case of imperfect crab, ICM, and channel calibration.

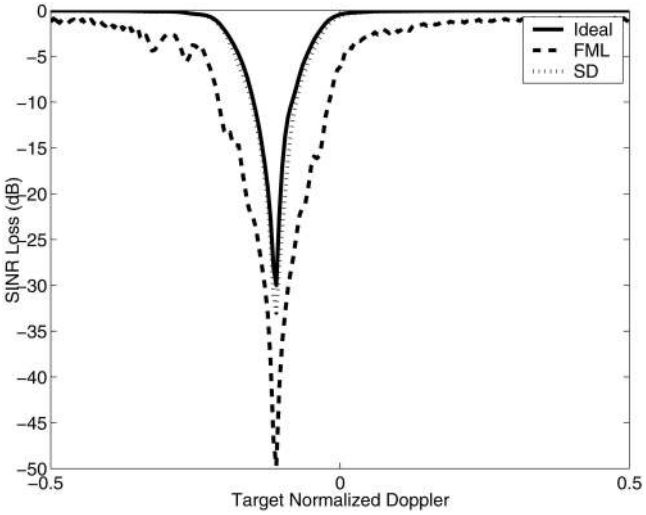

Fig. 9. Average SINR loss for case of mismatched crab angle that has been corrected with real-time data.

7 to Fig. 8, it can be concluded that most of the degradation in performance is due to the imperfect knowledge of crab angle with some additional degradation due to the imperfections in ICM and channel mismatch. When crab angle is accurate, spectral-domain averaging seems to perform very well.

C. Correcting Scenario Parameters with Real-Time Data

Finally, we demonstrate that it may be possible to correct some knowledge errors using real-time data. The simulation used to generate Fig. 5 was repeated; however, crab angle was estimated from the datacube. First, a traditional sample covariance matrix was computed using sample support from only 40 range bins. This matrix was used to locate the clutter ridge in the angle-Doppler domain by computing the crab angle that would be required in order to produce the location of the estimated clutter ridge. This crab estimate was then used in calculating the space-time steering vectors.

Unfortunately, a simple Fourier-based estimate of the clutter spectrum is not sufficiently accurate. Therefore, 2-D superresolution has been applied to locate the clutter ridge in angle and Doppler. The sample covariance matrix was divided into clutter+noise and noise-only subspaces by estimating the clutter rank via Brennan's rule [1]. Next, the noise-only covariance matrix, $\mathbf{R}_n$, was formed from the noise-only subspace, and the angle-Doppler MUSIC [30] spectrum was calculated as

$$S_c(f_x, f_D) = \frac{1}{\mathbf{s}(f_x, f_D)^H \mathbf{R}_n \mathbf{s}(f_x, f_D)} \tag{17}$$

where $\mathbf{s}(f_x, f_D)$ is the hypothesized steering vector for spatial frequency f_x and Doppler frequency f_D. Once the angle-Doppler clutter spectrum is obtained from (17), the brightest peaks in the spectrum are selected. The number of peaks chosen is less than the predicted clutter rank. Finally, the locations of those peaks are used to compute crab angle using a curve-fitting approach.

Even with the small sample support used to form the covariance estimate for superresolution, the crab estimates are very accurate. Note that the clutter-to-noise ratio (CNR) might be as high as 40–60 dB in a given range bin. Since clutter is the desired signal for the purpose of estimating crab, this superresolution problem has excellent SNR properties and leads to excellent crab estimates. For Fig. 9, the superresolution crab estimate was 3.5083°, which was sufficient for excellent results.

VI. CONCLUSIONS AND FUTURE WORK

In this paper, we have presented a new technique for estimating the interference covariance matrix for STAP. We have proposed that the range-Doppler domain is a natural domain for applying a priori knowledge since both the range-Doppler domain and many knowledge sources provide information as a function of position on the Earth's surface. Furthermore, clutter can be averaged over statistically homogeneous regions when averaged in the range-Doppler domain. This leads to better clutter estimates than traditional techniques since traditional techniques average clutter over range bins that are often quite statistically different from the RUT.

We have demonstrated that in the limit of perfect knowledge, spectral-domain averaging produces near-ideal performance. In practice, very accurate space-time steering vectors are required to make the transformation from the spectral domain to the measurement domain. An initial evaluation of the effects of errors in radar system parameters such as

platform crab angle, ICM, and channel calibration was presented, as well as an example of how real-time data could be used to obtain an accurate estimate of platform crab angle in order to restore accurate space-time steering vectors. Ultimately, the benefits of the proposed spectral-domain clutter averaging will depend on the ability to obtain precise, accurate knowledge of the radar parameters and scenario. Without this ability, the space-time steering vectors are inaccurate and the clutter spectrum estimate is incorrectly mapped into the measurement domain.

Significant future research is still required. The range-Doppler image formation should be extended to a space-time technique to allow moving targets to be excluded from the estimate of the clutter spectrum. Strong clutter discretes and slow targets might still corrupt the clutter estimate, but their impact will depend on the number of cells averaged within a homogeneous region. Also, the effects of jammers should be studied, as well as the integration of spectral-domain averaging into the FML technique with assumed clutter covariance (FMLACC) of [15]. Finally, the impacts of other sources of error need to be quantified.

ACKNOWLEDGMENT

We are grateful to Nikhil S. Rajguru for coding the Sobel edge detector used in our work.

REFERENCES

[1] Ward, J.
Space-time adaptive processing for airborne radar.
Technical Report 1015, MIT Lincoln Laboratory, Lexington, MA, Dec. 1994.

[2] Guerci, J. R.
Space-Time Adaptive Processing for Radar.
Boston, MA: Artech House, 2003.

[3] Melvin, W. L.
A STAP overview.
IEEE AES Systems Magazine, **19**, 1 part 2 (Jan. 2004), 19–35.

[4] Brennan, L. E., and Reed, I. S.
Theory of adaptive radar.
IEEE Transactions on Aerospace and Electronic Systems, **9**, 2 (Mar. 1973), 237–252.

[5] Brennan, L. E., Mallet, J. D., and Reed, I. S.
Adaptive arrays in airborne MTI.
IEEE Transactions on Antennas and Propagation, **AP-24**, 5 (1976), 607–615.

[6] Klemm, R.
Space-Time Adaptive Processing: Principles and Applications.
London: The Institute of Electrical Engineers, 1998.

[7] Reed, I. S., Mallett, J. D., and Brennan, L. E.
Rapid convergence rate in adaptive arrays.
IEEE Transactions on Aerospace and Electronic Systems, **10**, 6 (Nov. 1974), 853–863.

[8] Wang, H., and Cai, L.
On adaptive spatial-temporal processing for airborne surveillance radar systems.
IEEE Transactions on Aerospace and Electronic Systems, **30** (July 1994), 660–670.

[9] Peckham, C. D., and Haimovich, A. M.
Reduced-rank STAP performance analysis.
IEEE Transactions on Aerospace and Electronic Systems, **36**, 2 (2000), 664–676.

[10] Goldstein, J. S., and Reed, I. S.
Theory of partially adaptive radar.
IEEE Transactions on Aerospace and Electronic Systems, **33**, 4 (Oct. 1997), 1309–1325.

[11] Guerci, J. R., Goldstein, J. S., and Reed, I. S.
Optimal and adaptive reduced-rank STAP.
IEEE Transactions on Aerospace and Electronic Systems, **36**, 2 (Apr. 2000), 647–661.

[12] Barton, T. A., and Smith, S. T.
Structured covariance estimation for space-time adaptive processing.
In *Proceedings of ICASSP*, vol. 5, 2, 1997, 3493–3496.

[13] Li, Y., and Cheong, C. H.
Block Toeplitz with Toeplitz block covariance matrix for space-time adaptive processing.
In *Proceedings of the 2002 IEEE Radar Conference*, Apr. 2002, 363–368.

[14] Steiner, M. J., and Gerlach, K.
Fast converging adaptive processor for a structured covariance matrix.
IEEE Transactions on Aerospace and Electronic Systems, **36**, 4 (Oct. 2000), 1115–1126.

[15] Gerlach, K., and Picciolo, M. L.
Airborne/spacebased radar STAP using a structured covariance matrix.
IEEE Transactions on Aerospace and Electronic Systems, **39**, 1 (Jan. 2003), 269–281.

[16] Page, D., Scarborough, S., and Crooks, S.
Improving knowledge-aided STAP performance using past CPI data.
In *Proceedings of the 2004 IEEE Radar Conference*, Philadelpha, PA, Apr. 2004, 295–300.

[17] Bergin, J. S., Teixeira, C. M., Techau, P. M., and Guerci, J. R.
STAP with knowledge-aided data pre-whitening.
In *Proceedings of the 2004 IEEE Radar Conference*, Philadelpha, PA, Apr. 2004, 289–294.

[18] Capraro, C. T., Capraro, G. T., Weiner, D. D., Wicks, M. C., and Baldygo, W. J.
Improved STAP performance using knowledge-aided secondary data selection.
In *Proceedings of the 2004 IEEE Radar Conference*, Philadelphia, PA, Apr. 2004, 361–365.

[19] Melvin, W. L., et al.
Knowledge-based space-time adaptive processing for AEW radar.
IEEE AES Systems Magazine, **13**, 4 (Apr. 1998), 37–42.

[20] Goodman, N. A., and Gurram, P. R.
STAP training through knowledge-aided predictive modeling.
In *Proceedings of the 2004 IEEE Radar Conference*, Philadelphia, PA, Apr. 2004, 388–393.

[21] Zywicki, D. J., Melvin, W. L., Showman, G. A., and Guerci, J. R.
STAP performance in site-specific clutter environments.
In *Proceedings of the 2003 IEEE Aerospace Conference*, vol. 4, Mar. 8–15, 2003, 2005–2020.

[22] Zywicki, D. J., and Melvin, W. L.
Application of cultural databases in site-specific clutter modeling.
In *Proceedings of 2002 Knowledge-Aided Sensor Signal Processing and Expert Reasoning (KASSPER) Workshop*, Washington, D.C., Apr. 3, 2002, CD ROM.

[23] Zatman, M.
Circular array STAP.
IEEE Transactions on Aerospace and Electronic Systems, **36**, 2 (Apr. 2000), 510–517.

[24] *Proceedings of the 2002 Knowledge-Aided Sensor Signal Processing and Expert Reasoning (KASSPER) Workshop*, Washington, D.C., Apr. 3, 2002, CD ROM.

[25] Guerci, J. R.
Theory and application of covariance matrix tapers for robust adaptive beamforming.
IEEE Transactions on Signal Proceedings, **47**, 4 (Apr. 1999), 977–985.

[26] Guerci, J. R., and Bergin, J. S.
Principle components, covariance matrix tapers, and the subspace leakage problem.
IEEE Transactions on Aerospace and Electronic Systems, **38**, 1 (Jan. 2002), 152–162.

[27] Techau, P. M., Bergin, J. S., and Guerci, J. R.
Effects of internal clutter motion on STAP in a heterogeneous environment.
In *Proceedings of the 2001 IEEE Radar Conference*, Atlanta, GA, May 1–3, 2001.

[28] Billingsley, J. B.
Exponential decay in windblown radar ground clutter Doppler spectra: Multifrequency measurements and model.
Technical Report 997, MIT Lincoln Laboratory, Lexington, MA, July, 1996.

[29] Gonzalez, R. C., and Woods, R. E.
Digital Image Processing (2nd ed.).
Englewood Cliffs, NJ: Prentice-Hall, 2002.

[30] Schmidt, R. O.
Multiple emitter location and signal parameter estimation.
IEEE Transactions on Antennas and Propagation, **34** 3 (Mar. 1986), 276–280.

Prashanth R. Gurram was born in Hyderabad, India, on August 18, 1979. He received the B.S. degree in electrical engineering in 2002 from the Osmania University College of Engineering, Hyderabad, India and the M.S. degree in electrical engineering in 2006 from the University of Arizona, Tucson.

He worked as an intern for Qualcomm Inc. from 2005 to 2006 and now works for Qualcomm as a DSP firmware engineer.

Nathan A. Goodman (S'98—M'02) received the B.S., M.S., and Ph.D. degrees in electrical engineering from the University of Kansas, Lawrence, in 1995, 1997, and 2002, respectively.

He is currently an assistant professor with the Department of Electrical and Computer Engineering at the University of Arizona. Within the department, he directs the Laboratory for Sensor and Array Signal Processing. From 1996 to 1998, he was an RF systems engineer for Texas Instruments, Dallas, TX, and from 1998 to 2002, he was a graduate research assistant in the Radar Systems and Remote Sensing Laboratory at the University of Kansas. His research interests are in radar and array signal processing.

Dr. Goodman was awarded the Madison A. and Lila Self Graduate Fellowship from the University of Kansas in 1998. He was also awarded the IEEE 2001 International Geoscience and Remote Sensing Symposium Interactive Session Prize Paper Award.